

Effects of rapid thermal annealing on the optical properties of low-loss 1.3 μm GaInNAs/GaAs saturable Bragg reflectors

H. D. Sun,^{a)} R. Macaluso, S. Calvez, G. J. Valentine, D. Burns, and M. D. Dawson
Institute of Photonics, University of Strathclyde, 106 Rottenrow, Glasgow G4 0NW, United Kingdom

K. Gundogdu, K. C. Hall, and T. F. Boggess
Department of Physics & Astronomy, The University of Iowa, Iowa City, Iowa 52242

T. Jouhti and M. Pessa
Optoelectronics Research Centre, Tampere University of Technology, P. O. Box 692, FIN-33101 Tampere, Finland

(Received 18 November 2003; accepted 10 May 2004)

We report studies of the effect of rapid thermal annealing (RTA) on the optical properties of a low-loss 1.3 μm saturable Bragg reflector (SBR), consisting of a GaInNAs/GaAs single quantum well embedded in an AlAs/GaAs Bragg reflector grown monolithically on a GaAs substrate. RTA gives rise to a blueshift of the photoluminescence (PL) peak (and therefore of the excitonic absorption peak) and an enhancement of PL intensity, while the reflectivity properties including peak reflectivity and bandwidth are not degraded. Temperature dependent photoluminescence measurements show that the RTA-induced blueshift of photoluminescence consists of two components: one originating from the increase of optical transition energies and another from the reduction of carrier localization. Time-resolved photoluminescence results at room temperature provide information about the recombination dynamics of carriers directly relevant to the application of the SBR in laser mode locking. © 2004 American Institute of Physics.

[DOI: 10.1063/1.1767612]

I. INTRODUCTION

Semiconductor saturable absorber mirrors are attractive elements for the generation of ultrashort pulses in mode-locked lasers because of their low cost, fast response, compactness, broad spectra coverage, and especially the advantage that the properties of these semiconductor structures can be custom designed and adapted to the requirements of solid-state lasers.¹ Demonstrated structures include the antiresonant Fabry-Perot saturable absorber² and the saturable Bragg reflector³ (SBR). A SBR comprises a semiconductor quantum well as saturable absorber within a single distributed Bragg reflector (DBR) stack⁴ and has the advantage that no postgrowth ion implantation or growth under nonstandard conditions is required. These factors allow very low nonsaturable loss structures to be produced in a single process. Since the first report of SBR (Ref. 4) for laser mode locking, these devices have drawn increasing attention for applications in various ultrafast solid-state lasers.^{5–8}

The generation of picosecond and femtosecond pulses from lasers around 1.3 μm is of great significance. Important categories of solid-state and semiconductor lasers have transitions in this wavelength region, including Nd-based lasers in various host crystals, vibronic lasers such as Cr:forsterite, and diode lasers and diode-pumped semiconductor lasers. Furthermore, this is an important wavelength window for optical fibre communications and is suitable for other uses such as frequency doubling to the red for projection displays.

In this wavelength range, GaAs/AlAs or GaAs/AlGaAs quarter-wave stacks on a GaAs substrate enable advantageous DBRs due to the lattice match and high refractive index contrast between AlAs and GaAs. However, as is widely known, conventional active materials in this wavelength range are based on InP-compatible materials (InGaAsP, AlGaInAs), not compliant with GaAs substrates. Unfortunately, InP-based Bragg stacks are not ideal for this wavelength range because of the limited refractive index contrast. Therefore complicated wafer-bonding techniques have been employed to integrate the InP-based quantum wells with GaAs-based Bragg reflectors.⁷ InGaAs/GaAs quantum wells were naturally proposed as an approach to construct monolithic SBRs on GaAs substrate, and were tried in self-starting mode-locked femtosecond Cr:forsterite lasers.^{5,6} However, in order to tune the excitonic absorption peak to the specified long wavelength, high In content is needed to be introduced beyond the critical strain-thickness limit for pseudomorphic growth, resulting in surface degradation and decrease in reflectivity. This critically increases the background nonsaturable loss, and thus increases the pump threshold and decreases the damage threshold of SBRs. To achieve low loss, suitable buffer layers or strain compensated structures have been employed to relieve the strain,^{5,6,8} but with increase in the complexity of growth and also giving rise to extra optical loss. Therefore it is desirable to have suitable materials compatible to GaAs substrate with band-gap fitting around 1.3 μm .

In recent years, GaInNAs/GaAs dilute alloys and related quantum well structures have been recognized as promising active materials in the 1.3–1.6 μm range.^{9,10} The large bow-

^{a)}Author to whom correspondence should be addressed; electronic mail: handong.sun@strath.ac.uk

ing coefficient due to the incorporation of N decreases the In content required to achieve a specific band gap. The advantages associated with this material system include the improved thermal characteristics, resulting from the larger conduction band offset (thus giving strong electron confinement) and a low temperature rate of change of band-gap energy, and the fact that GaInNAs can be coherently grown on GaAs substrates and so integrated monolithically with Bragg reflectors composed of AlAs/GaAs or AlGaAs/GaAs stacks. With these advantages, GaInNAs has drawn intensive attention for both planar structures and vertical cavity surface emitting lasers.^{11–17} Recently, we have reported a new application of GaInNAs/GaAs as a monolithic low-loss SBR, which has been used to generate high-power picosecond laser pulses in 1.3 μm mode-locked lasers.¹⁸ This concept has also been extended to 1.55 μm .¹⁹ We found that rapid thermal annealing provided a flexible way to tune the absorption wavelength of the SBR to fit specific lasers—fitting in nicely with the broad DBR bandwidth achievable in GaAs/AlAs mirrors—and was favorable for mode locking of high power lasers.¹⁸ In this paper, we present the detailed studies of the effect of RTA on the properties of this kind of SBR, which are important in deeper understanding of the mode-locking process. While the absorption wavelength demonstrates a significant blueshift under RTA, the reflectivity band of SBR hardly changes and the maximum reflectivity does not degrade. By investigating the temperature dependence of photoluminescence (PL) for as-grown and annealed samples, we can clearly separate the contributions of the decreased carrier localization effect and increased band gap to the blueshift of the PL energy. Time-resolved PL measurements are also performed for as-grown and annealed samples at room temperature by using a nonlinear up-conversion gating technique. It is found that the PL decay time is increased remarkably by RTA, which provides direct evidence that RTA decreases the nonradiative centers effectively. The related studies are significant for the design and application of not only SBR but also other GaInNAs-based devices including VCSELs.

II. EXPERIMENT

The 1.3 μm GaInNAs SBR was designed to give a high-reflectivity stop band centered at ~ 1320 nm employing standard transfer-matrix-type calculations. The structure of the SBR and its relative refractive index profile are plotted in Fig. 1(a). The Bragg reflector consists of 26 periods of GaAs (115 nm)/AlAs (97 nm) quarter-wave layers grown on a GaAs substrate. A nominally 7 nm thick $\text{In}_{0.35}\text{Ga}_{0.65}\text{As}_{0.981}\text{N}_{0.019}$ single quantum well was embedded centrally within the topmost GaAs layer as a saturable absorber. The sample was grown by solid-source molecular beam epitaxy on a 2 inch GaAs substrate. A radio-frequency-coupled nitrogen plasma source was used to generate reactive nitrogen species for the GaInNAs quantum well (QW). To enable as versatile a structure as possible, our SBR was deliberately grown with no *in-situ* annealing, allowing for the possibility of selected postgrowth annealing treatment. As-grown wafer looked mirror-smooth, and the cross section SEM shown in Fig. 1(b) demonstrates clear interfaces be-

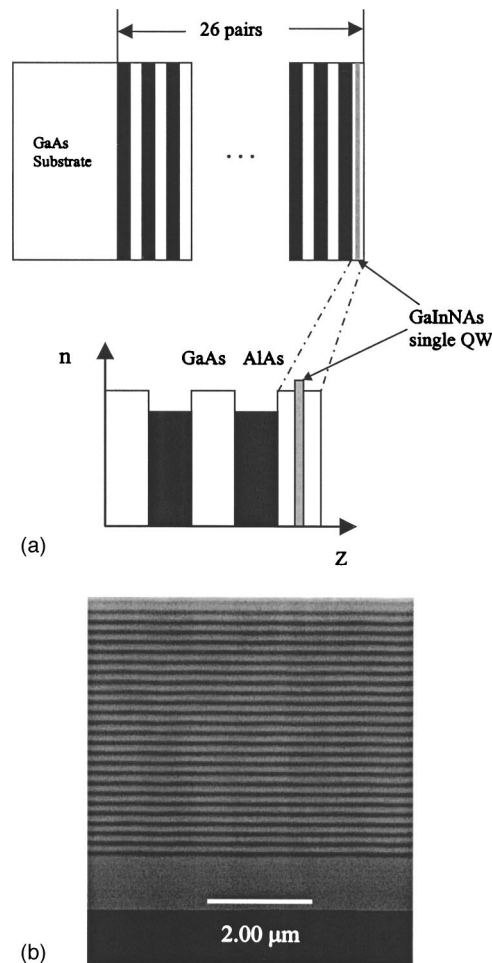


FIG. 1. (a) Saturable Bragg reflector structure and refractive index profile for a stack of AlAs/GaAs mirror pairs on a GaAs substrate and a single GaInNAs quantum well buried in the top layer, and (b) SEM cross section of the mirror structure.

tween the layers. The effect of RTA on the SBR was investigated by optical spectroscopy including PL, reflectivity, and time-resolved PL (TRPL), both before and after RTA. During the RTA process, the samples were kept in a flowing nitrogen ambient, and a GaAs wafer covered the surface to protect the samples.

(PL) was excited by a high power 670 nm diode laser. Depending upon the requirements, two kinds of light-collecting geometry were employed. In the backscattering geometry, both the excitation and PL signal collection are in the direction normal to the sample surface; in the edge-emitting geometry, the excitation is in the normal direction while the PL signal is collected in the edge direction. The collected PL signal was dispersed by a 0.46 m grating monochromator and detected by a thermoelectrically cooled InGaAs detector using standard lock-in techniques. Variable-temperature capability (5–300 K) was provided by a liquid He cooled cryostat.

(TRPL) measurements were performed using 140 fs pulses with repetition frequency of 76 MHz from a mode-locked Ti:sapphire laser tuned to 825 nm. The PL from the GaInNAs QW was up-converted in a 0.5 mm thick LiIO₃ crystal, with a system temporal resolution of ~ 200 fs and a

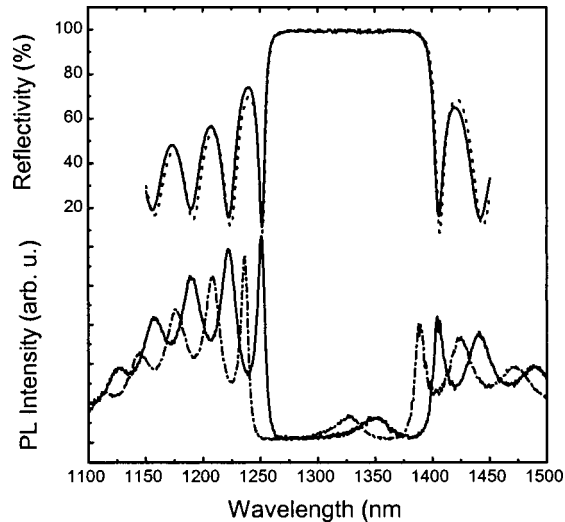


FIG. 2. A typical spectrum of low intensity reflectivity of an as-grown saturable Bragg reflector (upper trace). The lower traces show the typical PL spectra at room temperature measured at the central (solid curve) and an edge point (dotted curve) in the wafer in backscattering geometry.

10 meV spectral resolution.²⁰ The TRPL measurements were performed at room temperature at the PL peak of GaInNAS QW.

III. RESULTS AND DISCUSSION

The upper trace in Fig. 2 shows the low-intensity reflectivity spectrum of the SBR structure measured at the center of the wafer. The spectral width of high reflectivity stop-band region is larger than 120 nm, which results from the high refractive index contrast between AlAs and GaAs. The reflectivity spectrum calculated by the transfer-matrix method is plotted in the same figure (dotted curve). It can be seen that the measured reflectivity is closely consistent with the design. The lower traces in Fig. 2 show typical PL spectra at room temperature measured at the central (solid curve) and an edge point (dash-dot curve) in the wafer in backscattering geometry. The PL from the quantum well is located in the high reflectivity band of the Bragg reflector with peak wavelengths of 1351 (center) and 1326 nm (edge), respectively. The assignment of these features to quantum well emission was confirmed by temperature dependent measurements, whereby the different rate of wavelength shift of quantum well and mirror features are readily distinguishable (further confirmation by PL measurement observed in the edge-collection geometry as will be discussed later, because in such a situation the PL spectrum is barely modulated by the SBR reflectivity). The PL spectra recorded display a strongly modulated signal outside the high reflectivity stop band of the SBR. It is interesting to note that the backscattering PL spectrum also displays an inverted mirror reflectivity characteristic. This is attributed to the DBR filtering the long-wavelength PL tail of light generated in the GaAs layers in the structure. It has the attractive consequence that a single measurement of backscattering PL provides information on both the reflectivity band (associated with Bragg stack) and the relative position of the absorption wavelength (associated with quantum well).

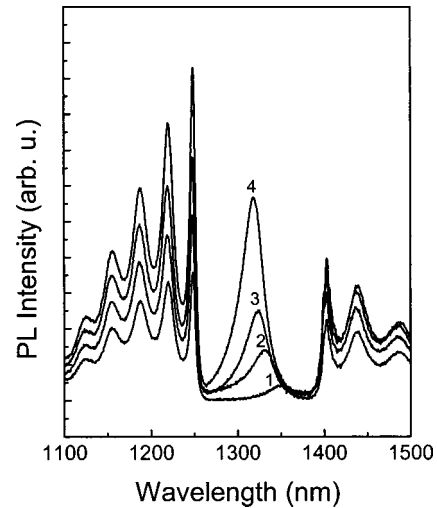


FIG. 3. PL spectra of SBR samples annealed at 700°C for different times: (1) as-grown, (2) 10 s, (3) 30 s, (4) 90 s.

The difference in the PL energies at different points originates from the (small) nonuniformity of layer thickness in the wafer. The PL mapping pattern is symmetric about the center and the layer thickness decreases from center to edge. Therefore both the PL peak and the Bragg stop-band shift to shorter wavelength. However, the blueshift of the QW PL peak due to the change in quantum confinement is expected to be larger than that of the reflectivity band which changes linearly with thickness. As shown in Fig. 2, the PL peak wavelength shifts about 25 nm from center to edge while the Bragg reflectivity band blueshifts only about 16 nm.

As is well known, the SBR mode-locking mechanism is dominated by the dynamic changes that occur near the excitonic absorption peak in the quantum well. The performance of mode locking with SBR is sensitive to the relative position of the operation wavelength to the exciton absorption peak. The optimum operation wavelength is generally close to or slightly above the exciton absorption peak.² Therefore, for mode-locking applications, the as-grown wafer can only cover wavelength from 1326 to 1351 nm. In order to extend the usefulness of this SBR to achieve high mode-locking performance for the widest range of Nd-doped lasers, including Nd:YLF with operating wavelength of 1314 nm, it is desirable to further blueshift the excitonic absorption peak wavelength. Although the band gap of the quantum well may be tuned by lowering the temperature, the requirement for cooling and temperature control is disadvantageous for practical application. Here, we employ RTA to shift the optical band gap, which has been proved to be an effective method.

To optimize the annealing conditions, we have performed RTA at different temperatures for various times. Considering the reflectivity and PL peak wavelength shift, the optimal temperature is determined to be around 700°C. Figure 3 shows the typical PL spectra of the samples annealed at 700°C for different times. The effect of RTA on the PL properties is clear, represented by the blueshift of PL peak and the enhancement of PL intensity (spectra 1–4). The PL features of samples annealed at 700°C as a function of annealing time are summarized in Fig. 4. With the increase of

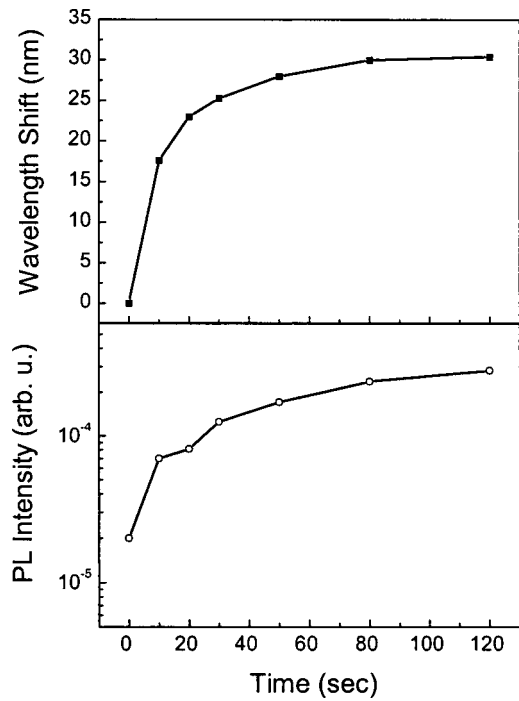


FIG. 4. Dependence of PL intensity and wavelength shift on annealing time at 700°C.

the annealing time, the emission shifts progressively to shorter wavelength while the emission intensity increases significantly. This evolution does not end for up to 120 s, although it shows the tendency of saturation for longer time annealing. These results are in good agreement with other reports.²¹⁻³¹ It is worth noting that while the PL peak has been clearly affected by the annealing process the reflectivity band is hardly changed by the same process and there is no observable decrease in reflectivity. This implies that at 700°C, the RTA process does not degrade the reflective properties, which is an important factor in practical applications.

To understand the influence of RTA on the optical properties of the SBR, we performed temperature-dependent PL measurements on both an unprocessed SBR sample and one annealed sample at 700°C for 80 s. Figure 5(a) shows the PL spectra of the as-grown SBR sample at different temperatures. With the decrease of temperature, the PL intensity increases rapidly, and the PL peaks shift to shorter wavelength. As can be seen, while the PL peak shifts to shorter wavelength, the reflectivity band also has a small blueshift with temperature. The blueshift of the PL peak results from the band-gap increase by the decrease of temperature, while the shift of reflectivity band is due to the thickness contraction (and refractive index change) induced by the temperature decrease. However, the rate of blueshift of the PL peak is much greater than that of the mirror, consistent with common observations in semiconductor microcavities. For example, when the temperature decreases from 290 to 15 K, the PL peak blueshifts by 82.5 nm, while the reflectivity stop band blueshifts only about 11.5 nm. So at low temperature, the QW PL peak gets closer to the mirror stop-band edge. This causes a difficulty with the measurement on the annealed

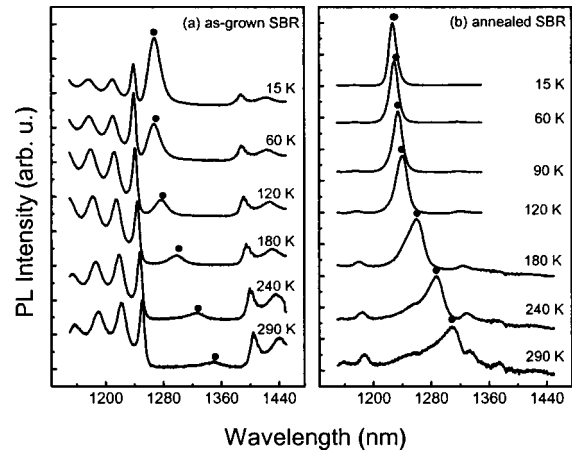


FIG. 5. Temperature dependent PL spectra of an as-grown SBR device measured in backscattering direction (a) and a SBR device annealed at 700°C for 80 s measured in edge direction (b).

sample. Since RTA shifts the PL from the quantum well close to the stop-band edge, the PL of QW will merge into the resonant peak at low temperature. Therefore it is impossible to identify the PL peak at low temperature with backscattering measurements. To circumvent this difficulty we measured the PL in the edge geometry at various temperatures. The result is shown in Fig. 5(b). In this situation, the PL is dominated by the PL signal due to GaInNAs quantum well emission and other signals outside the reflectivity band are largely eliminated.

Figure 6 shows the dependence of PL peak energies of the as-grown and annealed samples on temperature as shown in Fig. 5. It is noted that for annealed sample the PL keeps shifting to lower energy as the temperature increases, which is normal behavior for a semiconductor. However, for the as-grown sample, the PL first blueshifts (from 15 to 40 K) and then redshifts. This feature is typically recognized as an

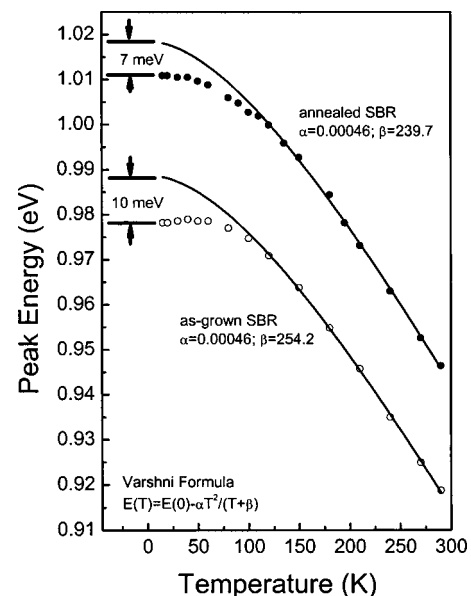


FIG. 6. Temperature dependence of experimental PL peak energies of an as-grown SBR device (closed circles) and a SBR annealed at 700°C for 80 s (open circles). The solid curves represent the fitting according to Varshni equation.

indication of carrier (exciton) localization. Actually, carrier localization is a ubiquitous phenomenon for GaInNAs/GaAs QWs and shows different detailed low-temperature features depending on the distribution of the localized states.³² But at higher temperatures (over 100 K) the PL properties should be governed by delocalized states, which can be described by Bose-Einstein formulas or more often by the Varshni empirical equation³³ as follows:

$$E(T) = E(0) - \frac{\alpha T^2}{T + \beta},$$

where $E(0)$ represents the band gap at 0 K, α and β are the fitting parameters. We have fitted the temperature dependence of the PL energies according to the above equation. At high temperatures, the experimental PL energies agree well with the Varshni equation. Least-squares fitting gives the fitting parameters α and β as 4.6×10^{-4} eV/K and 254.2, respectively, for as-grown sample, and 4.6×10^{-4} eV/K and 239.7 for the annealed sample. This implies that the band gaps of both samples have similar temperature dependence, except that the optical band gap has an increase of about 30 meV after annealing. However, as the temperature decreases, the PL energies gradually deviate from the Varshni equation. The difference of PL energies between the experiment and theory at the lowest temperature represents the depth of localization. The localization energies before and after the annealing are 10 and 7 meV, respectively. This indicates that the annealing process gives rise to the reduction of localization and a blueshift of PL energy of 3 meV at low temperature.

The blueshift phenomenon induced by annealing in dilute-nitride-arsenides has been investigated extensively, but the related mechanisms are still controversial.^{21–31} One of the explanations is that the blueshift of PL was related to the improvement of the alloy uniformity or decreased localization effect.^{21,22} This picture can only explain the blueshift of PL at low temperature, and predicts no blueshift at room temperature because the band gap has actually not changed. Another explanation is that the RTA-induced blueshift originates from the increase of the band gap of the QWs.^{23–31} Obviously, it is impossible to resolve the two effects induced by RTA (reduction of localization and increase of band gap) merely by low temperature or room temperature PL measurements. By investigating the temperature dependence of PL, however, we can clearly separate them from each other. In our experiment, both effects have been observed, but the increase of band gap is the main mechanism. This is the key to the tunability of the SBR for mode locking. With respect to the mechanisms of the RTA-induced increase of band gap, it has been proposed that RTA may lead to the interdiffusion of As-N (Refs. 23–25) or Ga-In (Refs. 26 and 27) between the QWs and barriers. Recently, it has been proposed that annealing promotes a change of N-bonding configuration from a Ga-rich to an In-rich environment and therefore increases the band gap which results in a blueshift of PL.^{28–31} As a matter of fact, detailed studies on QWI in GaInNAs/GaAs MQWs by some of the authors have shown that QWI is induced by the interdiffusion of In-Ga between QWs and barriers rather than As-N, and the diffusion is ob-

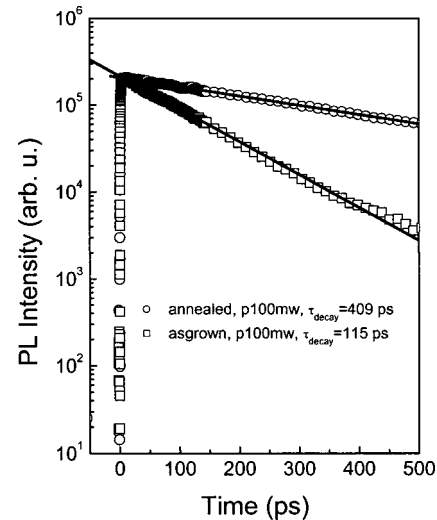


FIG. 7. Time-resolved PL intensity for an as-grown SBR (open squares) and a SBR annealed at 700°C for 80 s (open circles). The solid curves represent the fitting using a single exponential decay function. The time constant τ_{decay} has been denoted in the figure.

servable only when point defects are introduced.³⁴ Experiments of N-concentration dependent QWI provide supportive evidence of a bond configuration change from Ga-N to In-N.³⁵

Although the enhancement of PL intensity in GaInNAs or GaNAs is well recognized to result from the removal of nonradiative recombination centers by thermal annealing, the only experimental evidence is optically detected magnetic resonance studies.²² Time-resolved PL studies are an effective way to study the recombination dynamics. Buyanova *et al.* have performed TRPL measurements on GaNAs/GaAs multiquantum well structure at low temperature, but the result could not explain the strong increase of PL intensity at room temperature.²² Here we present our comparative measurements of TRPL on as-grown and annealed SBR samples at room temperature by the nonlinear up-conversion technique. Figure 7 shows the typical PL intensity evolution with time under an excitation power of 100 mW for an as-grown and an annealed sample. Similar to the observation of Härkönen *et al.* in a 1.5 μm SBR, (Ref. 36), the time decay profiles of PL can be fitted with one-exponential function. It is clearly seen that effective time constants with as-grown and annealed samples are 115 and 409 ps, respectively. We also performed TRPL measurements under different excitation powers and found that the effective time constant increases with the excitation power. Figure 8 shows the PL evolution of an annealed sample under the excitation power of 10 and 100 mW; the time constants are determined to be 231 and 409 ps, respectively. The inset of Fig. 8 illustrates the effective lifetime of as-grown and annealed samples as a function of excitation power. As is well known, the decay of PL in semiconductors is a dynamic process governed by competitive radiative and nonradiative recombination processes. The radiative and nonradiative lifetimes have different temperature dependences. The radiative lifetime increases as temperature increases while the tendency of the nonradiative lifetime is the converse. Therefore, at room

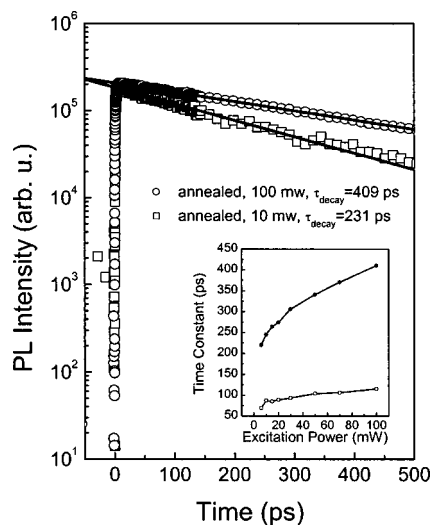


FIG. 8. Time-resolved PL intensity for an annealed SBR sample under the excitation power of 10 mW (open squares) and 100 mW (open circles), respectively. The inset shows the dependence of the time constant of an as-grown SBR device (closed squares) and a SBR device annealed at 700°C for 80 s (closed circles) on excitation power.

temperature, the nonradiative lifetime is shorter than the radiative lifetime, and the effective PL decay time is determined by the nonradiative lifetime which is dependent on the density of nonradiative recombination centers. When the excitation density is low, most of the excited carriers recombine through nonradiative channels. As the excitation density increases, a larger fraction of the carriers will recombine radiatively due to the saturation of nonradiative recombination channels, and therefore the effective lifetime will increase. The competitive recombination between the radiative and nonradiative channels can account for the monotonic increasing relation between the effective lifetime and excitation power, and reflects the saturation effect of nonradiative recombination. The significant increase of the decay time in the annealed sample implies the decrease of nonradiative recombination, which provides direct evidence that the defects induced by N ions in dilute-nitride-arsenides can be effectively cured by RTA. On the other hand, although RTA provides an effective approach for adjusting the absorption spectral band, it also increases the recovery time of the SBR which—depending on the particular laser system to be mode locked—may be undesirable for ultrafast photonics applications. In order to decrease the response time of SBR, other processes, such as ion implantation, may be needed.^{36,37}

IV. SUMMARY

In summary, we have studied the effect of rapid thermal annealing on the optical properties of a SBR for 1.3 μm mode-locked lasers which utilizes a GaInNAs/GaAs single quantum well as saturable absorber. RTA gives rise to both a blueshift of PL peak and an enhancement of PL intensity, as is the case for “bare” GaInNAs quantum wells. The samples with optimum annealing conditions show a blueshift of the PL peak of about 30 nm, while the reflectivity properties have been barely affected. Temperature dependent PL measurements show that the PL blueshift by RTA is mainly due

to the increase of band gap associated with the bond change of N from a Ga rich to an In-rich configuration. Time-resolved PL measurement by up-conversion techniques at room temperature has provided information about the recombination dynamics of both as-grown and annealed samples, and provides direct evidence that RTA effectively reduces the densities of nonradiative centers and therefore increases the PL efficiency. It has also been shown that while RTA is an effective way to tune the absorption band of a SBR to fit the mode-locking wavelength, it also increases the response time of SBR which may be a factor to consider in optimizing mode-locked laser performance.

ACKNOWLEDGMENT

This work was supported by the EPSRC “PHOTON” project and UK LINK-OSDA project “GAINS.”

- ¹U. Keller, *Appl. Phys. B: Lasers Opt.* **58**, 347 (1994).
- ²U. Keller *et al.*, *IEEE J. Sel. Top. Quantum Electron.* **2**, 435 (1996).
- ³S. Tsuda, W. H. Knox, S. T. Cundiff, W. Y. Jan, and J. E. Cunningham, *IEEE J. Sel. Top. Quantum Electron.* **2**, 454 (1996).
- ⁴S. Tsuda, W. H. Knox, E. A. de Souza, W. Y. Jan, and J. E. Cunningham, *Opt. Lett.* **20**, 1406 (1995).
- ⁵P. T. Guerreiro, S. Ten, E. Slobodchikov, Y. M. Kim, J. C. Woo, and N. Peyghambarian, *Opt. Commun.* **136**, 27 (1997).
- ⁶Z. Zhang, K. Torizuka, T. Itatani, K. Kobayashi, T. Sugaya, and T. Nakagawa, *Opt. Lett.* **22**, 1006 (1997).
- ⁷J. L. Shen *et al.*, *J. Opt. Soc. Am. B* **16**, 1064 (1999).
- ⁸D. Burns, M. Hetterich, A. I. Ferguson, E. Bente, M. D. Dawson, J. I. Davies, and S. W. Bland, *J. Opt. Soc. Am. B* **17**, 1 (2000).
- ⁹M. Kondow, K. Uomi, A. Niwa, T. Kitani, S. Watahiki, and Y. Yazawa, *Jpn. J. Appl. Phys., Part 1* **35**, 1273 (1996).
- ¹⁰I. A. Buyanova, W. M. Chen, and B. Monemar, *MRS Internet J. Nitride Semicond. Res.* **6**, 1 (2001).
- ¹¹T. Kitatani, M. Kondow, S. Nakatsuka, Y. Yazawa, and M. Okai, *IEEE J. Sel. Top. Quantum Electron.* **3**, 206 (1997).
- ¹²M. C. Larson, M. Kondow, T. Kitatani, K. Nakahara, K. Tamura, H. Inoue, and K. Uomi, *IEEE Photonics Technol. Lett.* **10**, 188 (1998).
- ¹³M. Kondow, Y. Kitani, K. Nakahara, and T. Tanaka, *Jpn. J. Appl. Phys., Part 2* **38**, L1355 (1999).
- ¹⁴T. Miyamoto, K. Takeuchi, F. Koyama, and K. Iga, *IEEE Photonics Technol. Lett.* **9**, 1448 (1997).
- ¹⁵S. Sato and S. Satoh, *Electron. Lett.* **35**, 1251 (1999).
- ¹⁶B. Borchert, A. Yu Egorov, S. Illek, M. Komanda, and H. Riechert, *Electron. Lett.* **35**, 2204 (1999).
- ¹⁷S. Calvez, A. H. Clark, J.-M. Hopkins, R. Macaluso, P. Merlin, H. D. Sun, and M. D. Dawson, *Electron. Lett.* **39**, 100 (2003).
- ¹⁸H. D. Sun, R. Macaluso, S. Calvez, G. J. Valentine, D. Burns, M. D. Dawson, T. Jouhti, and M. Pessa, *Opt. Lett.* **27**, 2124 (2002).
- ¹⁹O. G. Okhotnikov, T. Jouhti, J. Kontinen, S. Karirinne, and M. Pessa, *Opt. Lett.* **28**, 364 (2003).
- ²⁰L. Zhang, T. F. Bogess, D. G. Deppe, D. L. Huffaker, O. B. Sheekin, and C. Cao, *Appl. Phys. Lett.* **76**, 1222 (2000).
- ²¹L. Grenoiillet, C. Bru-Chevallier, G. Guillot, P. Gilet, P. Ballet, P. Duvaut, G. Rolland, and A. Million, *J. Appl. Phys.* **91**, 5902 (2002).
- ²²I. A. Buyanova, G. Pozina, P. N. Hai, N. Q. Thinh, J. P. Bergman, W. M. Chen, H. P. Xin, and C. W. Tu, *Appl. Phys. Lett.* **77**, 2325 (2000).
- ²³Z. Pan, L. H. Li, W. Zhang, Y. W. Lin, R. H. Wu, and W. K. Ge, *Appl. Phys. Lett.* **77**, 1280 (2000).
- ²⁴W. Li, J. Turpeinen, P. Melanen, P. Savolainen, P. Uusimaa, and M. Pessa, *Appl. Phys. Lett.* **78**, 91 (2001).
- ²⁵M. Albrecht *et al.*, *Appl. Phys. Lett.* **81**, 2719 (2002).
- ²⁶T. Kageyama, T. Miyamoto, S. Makino, F. Koyama, and K. Iga, *Jpn. J. Appl. Phys., Part 2* **38**, L298 (1999).
- ²⁷H. P. Xin, K. L. Kavanagh, M. Kondow, and C. W. Tu, *J. Cryst. Growth* **201**, 419 (1999).
- ²⁸S. Kurtz *et al.*, *Appl. Phys. Lett.* **78**, 748 (2001).
- ²⁹L. Largeau, C. Bondoux, G. Patriarche, C. Asplund, A. Fujioka, F. Salomonsson, and M. Hammar, *Appl. Phys. Lett.* **79**, 1795 (2001).

- ³⁰E. Tournié, M. A. Pinault, and A. Guzmán, *Appl. Phys. Lett.* **80**, 4148 (2002).
- ³¹V. Lordi, V. Gambin, S. Friedrich, T. Funk, T. Takizawa, K. Uno, and J. S. Harris, *Phys. Rev. Lett.* **90**, 115505 (2003).
- ³²H. D. Sun, M. Hetterich, M. D. Dawson, A. Yu. Egorov, D. Bernklau, and H. Riechert, *J. Appl. Phys.* **92**, 1380 (2002).
- ³³Y. P. Varshni, *Physica (Utrecht)* **34**, 149 (1967).
- ³⁴R. Macaluso, H. D. Sun, M. D. Dawson, F. Robert, A. C. Bryce, J. H. Marsh, and H. Riechert, *Appl. Phys. Lett.* **82**, 4259 (2003); H. D. Sun, R. Macaluso, M. D. Dawson, F. Robert, A. C. Bryce, J. H. Marsh, and H. Riechert, *J. Appl. Phys.* **94**, 1550 (2003).
- ³⁵H. D. Sun *et al.*, *J. Appl. Phys.* **94**, 7581 (2003).
- ³⁶A. Härkönen *et al.*, *Appl. Phys. A: Mater. Sci. Process.* **77**, 861 (2003).
- ³⁷M. J. Lederer *et al.*, *Appl. Phys. Lett.* **74**, 1993 (1999).